Photothermal heating of optically trapped gold nanoparticles quantified using controlled vesicle cargo release

Anders Kyrsting, Poul M. Bendix, and Lene B. Oddershede

Niels Bohr Institute, Blegdamsvej 17, 2100 Copenhagen, Denmark

ABSTRACT

Optically trapped metallic nanoparticles hold great promise as heat transducers in photothermal applications such as drug delivery assays or photothermal therapy. We use the heat dissipated from an optically trapped gold nanosphere to perform a controlled release of a fluorescently labeled vesicle lumen. In the assay, the ambient temperature is kept below the phase transition temperature of the vesicle. When the temperature reaches the phase transition temperature of the lipid, the vesicle becomes leaky and the fluorescently marked lumen diffuses out. We used gel phase vesicles as sensors to quantify the temperature profile around a nanoparticle optically trapped in three dimensions in a similar way as presented in Ref.[1] Trapping of 200 nm gold particles resulted in lower than expected heating, which may be accredited to the displacement of the particle from the optical focus due to high scattering forces experienced by the particle.

Keywords: Optical tweezers, gold nanoparticle, heating, photothermal therapy, giant unilamellar vesicles, lipid phase transition, surface plasmonics, Mie theory

1. INTRODUCTION

Gold nanoparticles are efficient as photothermal agents in the visual light range, as their surface plasmons resonate strongly with optical light. These nanoparticles can convey an intense local heating when irradiated near their optical resonance, which can be exploited in photothermal cancer therapy,[2] or in nano thermal substrate processing.[3] As phospholipid vesicles become permeable at their main phase transition,[4,5] they can be employed as thermally sensitive cargo vehicles for targeted delivery of active drugs or other biomolecules.[6–9] This can potentially be achieved by conjugating the gold nanoparticles to the surface of the vesicles, but precise measurement of the photothermal response for individual particles is required to control the vesicle volume release. The temperature increase in gold nanoparticles irradiated by resonant or off-resonant light has previously been profiled using 2D lipid assays, either by gold particles directly on vesicles[10] or on supported lipid bilayers.[11]

Here we show that the temperature response for a single gold nanoparticle, optically trapped in three dimensions, can be directly measured by quantifying the distance at which a trapped gold nanoparticle can induce a phase transition in a Giant Unilamellar Vesicle (GUV) and consequently induce leakage from the GUV. The assay is described in more detail in Ref.[1] The significant differences in heating efficiency for 200 nm gold particles determined in this assay and the previous 2D assay,[11] reveal that large gold nanoparticles are being displaced from the laser focus during 3D trapping. Furthermore, we show that the permeation out of the GUVs occurs simultaneously with the partitioning of a membrane-tethered fluorophore into the melted domain of the vesicles.

2. METHODOLOGY

As particles get smaller they tend to get increasingly difficult to confine in an optical trap, due to the decreasing electric polarizability which scales with volume of the particle. Metallic nanoparticles have a higher polarizability compared to polymer beads, stemming from mobile electron clouds which can oscillate in response to the trapping beam.[12] In this way, it is possible to trap individual metallic nanoparticles in a single beam trap.[13–16] In this work, the optical trap was based on a near IR 1064 nm wavelength Spectra Physics J201-BL-106C CW laser, implemented in a back port on a Leica SP5 confocal inverted microscope. For all experiments, a Leica PL APO NA 1.2 63x objective was used to both visualize the sample and for trapping.

Further author information: (Send correspondence to L.B.O.)
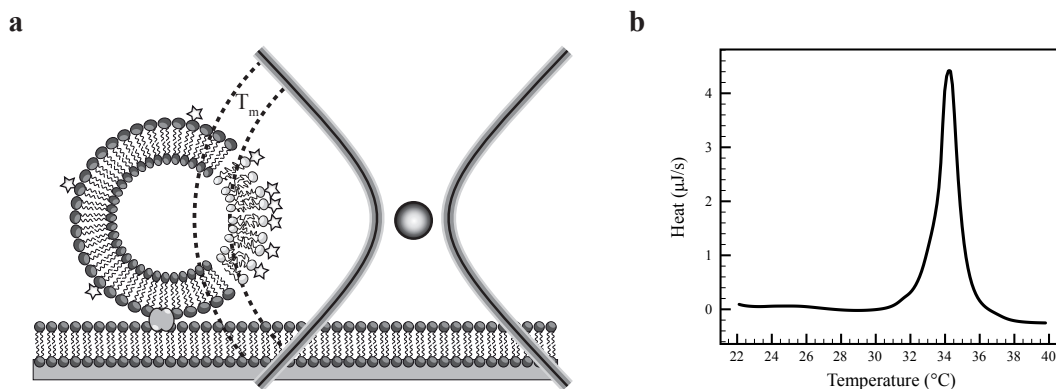
L.B.O.: E-mail: oddershede@nbi.dk

Figure 1. **a**: Illustration of the experimental setup, a GUV is immobilized on a supported lipid bilayer via biotin-streptavidin binding. The vesicle bilayer also contains Texas Red-DHPE lipids (stars). A single gold nanoparticle is held in an optical trap and the heat from photothermal conversion can melt a part of the distant vesicle. **b**: Calorimetric scan of 100 nm extruded $DC_{15}PC$ vesicles, showing a narrow lipid phase transition.

Gold nanoparticles from British Biocell International in the range 60 to 200 nm diameter were sonicated to minimize aggregates, and incubated with a thiolated polyethylene glycol polymer by Sigma Aldrich at a 9:1 volume ratio and agitated on a vortex shaker at 1000 rpm for 30 min. The aliquots were spun down and resuspended in Millipore water. This strongly reduces gold nanoparticle aggregation when working with aqueous buffers.

Supported lipid bilayers were prepared from powder stock by Avanti Polar Lipids, suspended in chloroform at 25 mg/mL, using a 100:1 molar ratio of 1-Palmitoyl-2-Oleoyl-sn-glycero-3-PhosphoCholine (POPC, no. 770557) and 1,2-dipalmitoyl-sn-glycero-3-PhosphoEthanolamine-N-biotinyl (Biotinyl-PE, no. 870277). 0.4 mL lipid solution was evaporated under a nitrogen flow in 5 mL glass vials and residual chloroform removed in a vacuum desiccator for 2 hours. The lipid film deposited in the vials was rehydrated in a 3 mL Phosphate Buffered Saline (PBS 10mM) containing 0.1M NaCl for 12 hours. The resulting vesicle suspension was extruded 9 times through a 100 nm pore size filter. This stock was added to piranha solution treated glass slides to form lipid bilayers coating the surface. To remove excess lipid material the glass slides were flushed extensively with Millipore water and subsequently with 10mM PBS containing 0.1M NaCl. The glass slides were assembled into samples using a circular teflon ring assembly pressed onto the glass, with a final sample volume of 500 μL. Neutravidin was added to the samples to a concentration of 0.2 μM and allowed to bind to the Biotinyl-PE for 5 min. before rinsing the sample with PBS.

GUVs were prepared from Avanti Polar Lipids stocks of 1,2-Dipentadecanoyl-sn-glycero-3-PhosphoCholine ($DC_{15}PC$, no. 850350), Biotinyl-DHPE, and 1,2-dihexadecanoyl-sn-glycero-3-PhosphoEthanolamine-Texas Red (TR-PE, no. T1395MP) by Invitrogen, at a ratio of 1000:1:30 in chloroform to a concentration of 25 mg/mL. Single droplets were placed in a custom Teflon container, allowed to evaporate for 30 min. under a gentle flow and finally left in a vacuum desiccator for 2 hours. The film was rehydrated in 0.2 M Sorbitol solution at 37°C, well above the lipid phase transition of 33-34°C, as shown in Figure 1b., for 3 hours with gentle shaking every half hour. The GUV suspension was cooled to RT and transferred to eppendorf tubes. The stock was only used for a week and stored at 5°C.

To load the GUVs with an easily detectable cargo, 10 μL Alexa Hydrazide 488 (Invitrogen) at 10 mg/mL in 0.1 M NaCl was mixed with 10μL GUV stock and heat cycled 3 times from 24°C to 37°C in 15 min. Immediately after, the filled GUVs were transferred to a waiting sample chamber and left to anneal for 30 min. Alexa 488 outside the GUVs was carefully washed away using PBS until the sample volume appeared clear, leaving surface tethered vesicles as shown in the illustration in Figure 1a. The fast transfer and gel phase vesicles resulted in spherical GUVs without major deformations.
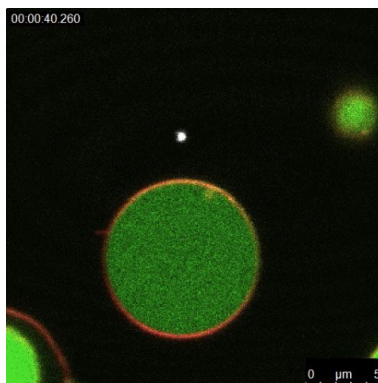
Figure 2. Video 1: Sample experiment. An unilamellar vesicle is approached by an optically trapped gold nanoparticle. When the heat from the gold particle (white dot) is sufficient to melt the tip of the membrane, the green (in video) Alexa 488 dye solution escapes the vesicle - at the same time a slight increase is measured in the membrane Texas Red signal. When the gold particle is removed, the membrane impermeability is reestablished. j wr⊲lf z0f qk0qti 13203339 1340, 5269903

Below and above the phospolipid main transition temperature, the vesicles are impermeable to the Alexa dye. At the transition, the vesicles become leaky due to the coexistence of fluid and gel phase domains and a decrease in the work needed to compress the bilayer laterally.[5] In this way, when a part of a GUV is melted, the Alexa 488 will diffuse out. The overall sample temperature was controlled within $\pm 0.5°$C and maintained at 8°C below the transition. On trapping a single gold nanoparticle, the trap was moved toward a vesicle at a constant speed of 10 nm/s using a piezo electric stage controller (Physik Instrumente, no. P5173CL).

All fluorophores and gold particles were visualized by using the confocal microscope in either fluorescence or reflection mode. The Texas Red-DHPE was excited at 594 nm and light was collected in the range 610-710 nm, while Alexa 488 was excited at 488 nm and emitted light collected at 495-565 nm - using photomultiplier tubes and acousto-optical beam splitter for detection. Backscattered light at 594 nm was used to visualize the gold nanoparticles. Movies were acquired at a frame-rate of 0.8 frames/s. During a typical experiment the trapped gold nanoparticle would approach the vesicle at 13 nm/frame, effectively sampling the approach sequence.

3. RESULTS

Using autofocus in order to find the equatorial plane of the vesicle, ensured that the vesicle would be approached in the shortest distance possible. This was necessary to minimize the error on the length measured between trapped particle and vesicle surface. As the gold nanoparticle is moved towards the vesicle, at some point a part of the vesicle bilayer will become fluidic because the heat released from the irradiated nanoparticle melts the membrane. This causes the green Alexa dye inside the vesicle to permeate the bilayer and diffuse away, as shown in Video 1.

The existence of both gel and fluidic areas of the bilayer causes a partitioning into the fluidic area by the Texas Red-DHPE lipid, as seen when comparing Figure 3a,b. This occurs at the same instant the Alexa begins to leak from the membrane, as can be seen in the area intensity plots in Figure 3c. Here, three separate experiments are shown, as the Alexa signal falls off; the membrane signal increases sharply - the coincidence of these two signal changes strongly support the claim that a local phase transition had occurred. As can be seen in Video 1, the membrane did not undergo violent undulations or rupture - ruptures were only rarely observed and are not included in the presented data. Bleaching was minimal and can be estimated from the initial near-flat slope in the Alexa signal; while the leakage induced drop-off appears linear. A control with a trapped gold nanoparticle inside a GUV, far away from the bilayer surface, showed no detectable bleaching, see Ref.[1] Hence, the fluorescent events shown in Figure 3c are not due to bleaching.

To quantify the melting distance between a gold nanoparticle and a GUV, we define the initial melting distance as corresponding to the time, t_m, when the two linear regimes for the Alexa signal intersect. The distance at $t = t_m$ was measured from the center of the lateral point spread function (PSF) of the gold nanoparticle orthogonally
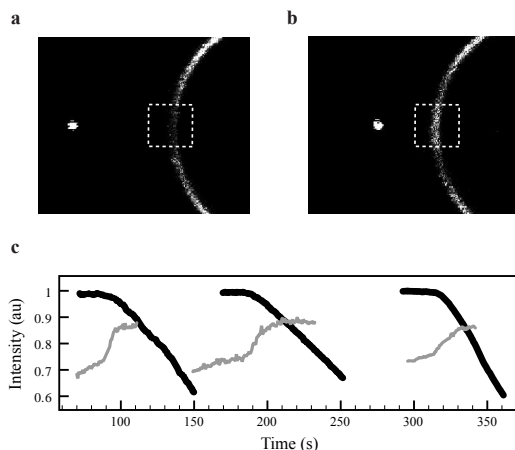
Figure 3. **a,b**: Confocal images from a typical experiment, only showing the trapped particle and the membrane signal. On moving the particle near the bilayer, a partitioning into the now melted area is seen for the membrane tethered dye. **c**: Area intensity plot for 3 experiments, the black line shows the Alexa 488 inside the vesicle; while the grey signal shows the increase in intensity of the boxed area in **a,b**.
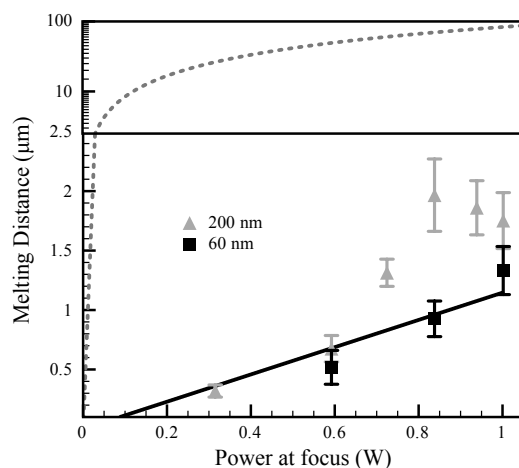

Figure 4. GUV melting distance as a function of laser intensity at the sample for gold nanoparticles with diameters of 60 nm and 200 nm. The lines show model expectations based on absorption cross sections calculated by Mie scattering and the focus point width, the full line shows the predicted melting distance for 60 nm particles, while the dotted line shows the predicted melting distance for 200 nm gold particles.

to the center of the nearest membrane signal. The melting distances for 60 and 200 nm gold particles trapped at laser powers between 315-1000 mW are shown in Figure 4. Each point represents an average of 5 individual experiments with error bars showing one standard deviation (SD).

The trapped gold nanoparticles can melt a bilayer at a distance exceeding by several orders of magnitude the diameter of the gold nanoparticle. In this case, the Goldenberg relation[17] describes the thermal flux in the system well, with a solution for the temperature increase at a given distance, s, outside the particle as

$$\Delta T(s) = \frac{AR^3}{3K_w s} \,. \tag{1}$$

Here, A is the energy input per volume, R the particle radius, and K_w the thermal conductivity of water. We calculate A as

$$A = IC_{abs}/V \,, \tag{2}$$

where I is the irradiance, C_{abs} the optical cross section of absorption, and V the particle volume. The optical cross sections of gold spherical nanoparticles irradiated by a 1064 nm laser beam can be described using Mie's theory.[18] The incident laser power on the particle can be estimated from the measured beam width of 800nm at the focus. The expected melting distance for gold nanoparticles can then be predicted as shown in Figure 4 for a 60nm (solid) and a 200nm (dotted) gold nanoparticle. For the 60 nm particle, this model is in very good agreement with the data points in Figure 4. However, for the 200 nm gold particles the model suggests melting distances an order of magnitude larger than the data. At the high laser powers needed to sustain stable trapping for the gold particles, Mie theory implies a plasma state for the 200 nm particles, if they trap at the center of the focus. Such extreme events or explosive boiling were, however, never observed. Since the large gold nanoparticles would be thermally unstable near the laser focus, with the laser powers used in this study, we expect these particles to be trapped in some local potential minimum having lower intensity and located away from the optical focus.

Using eq. 1 and the melting distances, the temperature response for the 60 nm gold particles was determined to be 523 K/W using a linear fit to the data, while a fit to the 200 nm particle data up to 0.83 W showed a response of 242 K/W.[1] Kotaidis et al. have shown heating by gold nanoparticles up to 80-90% of the critical temperature of water at 374°C without bubble formation.[19] This is the first measurements, to our knowledge, that directly show the temperature increase of single metal nanoparticles trapped in 3D. Bendix et al. recently showed that the temperature increase of gold particles trapped in 2D on a supported lipid bilayer is 385 K/W for 80 nm, 452 K/W for 100 nm, 732 K/W for 150 nm, and 1640 K/W for 200 nm, respectively[11] using a slightly larger focus than in the current study. Seol et al. estimated the heating of single 100 nm gold particles at 266 K/W, using the viscosity change in the medium as a probe for the surface temperature.[20] In the work by Seol et al. the temperature measurements rely on the calculations of the optical absorption cross section using the dipole approximation. The dipole approximation is only strictly valid for small spherical particles and underestimates the absorption at λ=1064nm for particles having d=100nm.

The presented work does not rely on calculated optical properties, but merely assumes the reciprocal relation between temperature and distance from the nanoparticle as show in eq. 1. Heating by the water-absorption is predicted to be on the order of 1 K/W,[21] thus small enough to be neglected as a heat-source in comparison to the heat produced by the trapped gold particles. The differences in heating response between 2D and 3D trapping are significant: the 60 nm particles trapped in 3D seem on a similar scale as presented in the 2D assay, while the 200 nm particle differs by a factor 7. In the 2D assay, particles were fixed in the axial direction, while they were free to move in z in this work. Furthermore, at high laser powers, the large particles would be launched away from the surface, suggesting they were not near their axial trapping equilibrium position. It should be noted that weaker trapping strengths for 200 nm gold particles have been reported, with some discussions of stability issues compared to smaller particles.[13, 16]

Turning to Mie theory, it is possible to theoretically examine the scattering properties of different sizes of particles. The calculated absorption and scattering cross sections, together with the total extinction for gold particles up to 200 nm in size can be seen in figure 5. It is evident that as particles get larger, scattering becomes the determining factor. This could partly explain the scaling observed for 60 and 200 nm particles: if the scattering cross section increases, one would expect an axial displacement from the trap focus in the classical optical tweezers model of gradient and scattering force. The gradient force relies on the electric polarizability of the particle, which can also be described by Mie theory as[22]

$$\alpha = i \left[\frac{3r^3}{2x^3} \cdot a_1 \right] , \tag{3}$$

where r is the particle radius and x the particle wave size factor as $x = 2\pi r/\lambda$. a_1 is the first electric scattering coefficient of the Mie solution.[18] To estimate the axial trapping position of the 60 and 200 nm gold particles, we look at the ratio between the two main determinants for the gradient force and the scattering force: the polarizability and the scattering cross section. As they both enter linearly into the force models, we propose the following relation as an initial estimate of the relative magnitude of optical forces:
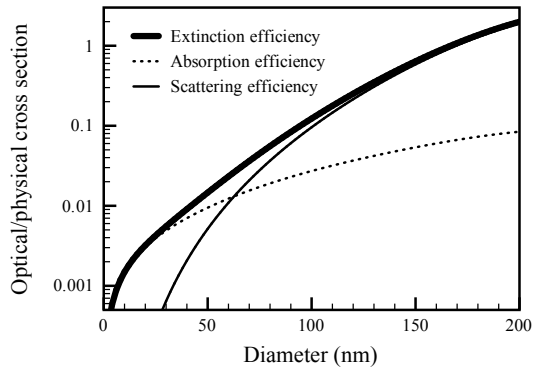
Figure 5. Optical cross sections divided by the physical cross section for gold particles up to 200 nm, interacting with a plane wave with $\lambda=1064$ nm. It can be seen that there exists a cross-over regime around 60 nm, where scattering begins to dominate over absorption.
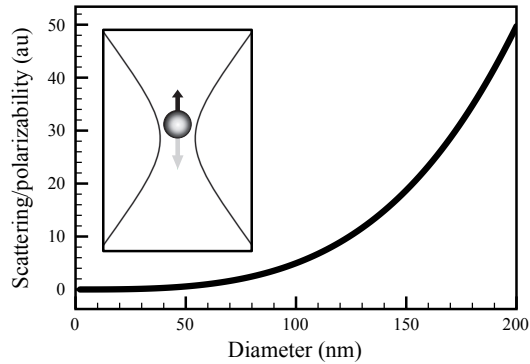

Figure 6. The ratio of the scattering cross section to polarizability for gold nanoparticles, rescaled to a value of 1 for 60 nm. Insert shows a cartoon of the forces on a given particle, grey arrows for gradient force and black arrows for scattering.

$$F_{s-p}(r) = \frac{C_{sca}(r)}{\alpha(r)} \ . \tag{4}$$

As can be seen in Figure 6, with increasing size comes an increasingly higher scattering cross section compared to the polarizability, suggesting better trapping for smaller particles near the center of the focus. Certainly this stops at a lower limit, when Brownian motion and focus intensity aberrations become major factors in trapping stability.[16] However, it is also apparent that there must be an upper limit for efficient axial trapping as this ratio continues to increase. Gold nanoparticles having d=200 nm trapped at the very focus have such high absorption cross sections, that they would turn into plasma according to Mie's equations for the intensities used here. At the same time they have even higher scattering cross sections as seen in Figure 5. The large radiation pressure on large particles combined with the melting distances we have measured, strongly support the idea that d=200nm gold nanoparticles cannot be trapped at the very focus of the laser beam but could potentially be displaced along the beam, as depicted in Figure 6.

4. CONCLUSION

We presented a new assay in which GUVs are used as thermal sensors to deduce the temperature of gold nanoparticles optically trapped in three dimensions. The heated nanoparticles induced a local phase transition in the GUV that can be imaged by phase sensitive chromophores having a preference for the more disordered

fluid phase. Moreover the local melting of the GUV bilayer permeabilizes the membrane and causes efflux of the entrapped fluorescent molecules when the local temperature reaches the lipid phase transition temperature. Therefore this assay allows us to efficiently probe the local temperature increase induced by optically trapped gold nanoparticles by two independent methods: membrane partitioning and membrane permeabilization. The temperature increase for gold nanoparticles trapped in 3D was measured for two particle sizes and showed large differences between the two sizes. Surprisingly, the temperature of the d=200 nm particles was lower than that of the 60 nm gold particles, in contrast to expectations based on Mie theory and assuming that the particles trap at the focal point. We propose, based on the temperature measurements and Mie's theory, that the 200 nm particles are axially displaced compared to the smaller 60 nm particles due to the much higher radiation pressure experience by the larger particles. The assay is envisioned to become a useful tool for quantifying the temperature response of any type of optically trapped particles and as a way to study well defined and stable phase domains in phospholipid bilayers.

5. ACKNOWLEDGEMENTS

REFERENCES

1. A. Kyrsting, P. M. Bendix, D. G. Stamou, and L. B. Oddershede, "Heat profiling of three-dimensionally optically trapped gold nanoparticles using vesicle cargo release.," *Nano Letters* , 2011.
2. A. Gobin, M. Lee, N. Halas, and W. James, "Near-infrared resonant nanoshells for combined optical imaging and photothermal cancer therapy," *Nano Letters* , 2007.
3. Y. Otani and N. Umeda, "Localized thermal processing with a laser-trapped and heated metal nanoparticle," *IEEJ Transactions on Electrical and Electronic Engineering* , 2007.
4. P.-Y. Bolinger, D. Stamou, and H. Vogel, "Integrated nanoreactor systems: triggering the release and mixing of compounds inside single vesicles.," *Journal of the American Chemical Society* , 2004.
5. A. Blicher, K. Wodzinska, and M. Fidorra, "The temperature dependence of lipid membrane permeability, its quantized nature, and the . . . ," *Biophysical Journal* , 2009.
6. D. Needham and M. Dewhirst, "The development and testing of a new temperature-sensitive drug delivery system for the treatment of solid tumors," *Advanced drug delivery reviews* , 2001.
7. D. Pissuwan, S. Valenzuela, and M. Cortie, "Therapeutic possibilities of plasmonically heated gold nanoparticles," *TRENDS in Biotechnology* , 2006.
8. C. Pitsillides, E. Joe, X. Wei, R. Anderson, and C. Lin, "Selective cell targeting with light-absorbing microparticles and nanoparticles," *Biophysical Journal* , 2003.
9. A. Angelatos, B. Radt, and F. Caruso, "Light-responsive polyelectrolyte/gold nanoparticle microcapsules," *J. Phys. Chem. B* , 2005.
10. A. Urban, M. Fedoruk, M. Horton, and J. O. Rädler, "Controlled Nanometric Phase Transitions of Phospholipid Membranes by Plasmonic Heating of Single Gold Nanoparticles," *Nano Letters* , 2009.
11. P. M. Bendix, S. N. S. Reihani, and L. B. Oddershede, "Direct measurements of heating by electromagnetically trapped gold nanoparticles on supported lipid bilayers.," *ACS nano* , 2010.
12. K. Svoboda and S. Block, "Optical trapping of metallic Rayleigh particles," *Optics letters* , 1994.
13. P. Hansen, V. Bhatia, N. Harrit, and L. Oddershede, "Expanding the optical trapping range of gold nanoparticles," *Nano Letters* , 2005.
14. C. Selhuber-Unkel, I. Zins, O. Schubert, and C. S. nnichsen, "Quantitative optical trapping of single gold nanorods," *Nano Letters* , 2008.
15. L. Bosanac, T. Aabo, P. Bendix, and L. Oddershede, "Efficient optical trapping and visualization of silver nanoparticles," *Nano Letters* , 2008.
16. F. Hajizadeh and N. Reihani, "Optimized optical trapping of gold nanoparticles," *Opt. Express* , 2010.
17. H. Goldenberg and C. Tranter, "Heat flow in an infinite medium heated by a sphere," *British Journal of Applied Physics* , 1952.

18. U. Kreibig, "Optical Properties of Metal Clusters," *Springer*, 1995.

19. V. Kotaidis, C. Dahmen, G. Von Plessen, F. Springer, and A. Plech, "Excitation of nanoscale vapor bubbles at the surface of gold nanoparticles in water.," *THE JOURNAL OF CHEMICAL PHYSICS*, 2006.

20. Y. Seol, A. Carpenter, and T. Perkins, "Gold nanoparticles: enhanced optical trapping and sensitivity coupled with . . . ," *Optics letters*, 2006.

21. S. Block, "Optical tweezers: a new tool for biophysics," *Modern cell biology*, 1990.

22. W. Doyle, "Optical properties of a suspension of metal spheres," *Physical Review B*, 1989.